Check for updates

Received: 3 May 2022 | Revised: 24 July 2022 | Accepted: 25 July 2022

DOI: 10.1002/pbc.29926

Pediatric Blood & Cancer

SIOP INTERNATIONAL SOCIETY OF PAEDIATRIC ONCOLOGY

aspho The American Society of Pediatric Hematology/Oncology

WILEY

ONCOLOGY: RESEARCH ARTICLE

Diverse mutations and structural variations contribute to Notch signaling deregulation in paediatric T-cell lymphoblastic lymphoma

Julia Salmerón-Villalobos[1,2,#] | Joan Enric Ramis-Zaldivar[1,2,#] | Olga Balagué[1,2,3] | Jaime Verdú-Amorós[4] | Verónica Celis[5] | Constantino Sábado[6] | Marta Garrido[7] | Sara Mato[1,2] | Javier Uriz[8] | M. José Ortega[9] | Angela Gutierrez-Camino[10] | Daniel Sinnett[10,11] | Unai Illarregi[12] | Máxime Carron[10] | Alexandra Regueiro[13] | Ana Galera[14] | Blanca Gonzalez-Farré[1,2,3] | Elias Campo[1,2,3] | Noelia Garcia[1] | Dolors Colomer[1,2,3] | Itziar Astigarraga[15,16] | Mara Andrés[17] | Margarita Llavador[18] | Idoia Martin-Guerrero[19,*] | Itziar Salaverria[1,2,*]

[1]Institut d'Investigacions Biomèdiques August Pi i Sunyer (IDIBAPS), Barcelona, Spain

[2]Centro de Investigación Biomédica en Red-Oncología (CIBERONC), Madrid, Spain

[3]Haematopathology Unit, Hospital Clínic, Barcelona, Spain

[4]Paediatric Oncology Department, Hospital Clínic, Valencia, Spain

[5]Paediatric Oncology Department, Hospital Sant Joan de Déu, Esplugues de Llobregat, Spain

[6]Paediatric Oncology Department, Hospital Vall d'Hebron, Barcelona, Spain

[7]Anatomic Pathology Department, Hospital Vall d'Hebron, Barcelona, Spain

[8]Paediatric Oncohaematology Department, Donostia University Hospital, Biodonostia Health Research Institute, San Sebastian, Spain

[9]Paediatric Oncology Department, Hospital Universitario Virgen de la Nieves, Granada, Spain

[10]Division of Haematology-Oncology, CHU Sainte-Justine Research Center, Montreal, Canada

[11]Department of Paediatrics, Faculty of Medicine, University of Montreal, Montreal, Canada

[12]Genetics, Physics Anthropology and Animal Physiology, Faculty of Science and Technology, UPV/EHU, Leioa, Spain

[13]Paediatric Haematology and Oncology Department, Hospital Clínico Universitario de Santiago de Compostela, Santiago de Compostela, Spain

[14]Paediatric Oncohaematology Department, Hospital Clínico Universitario Virgen de la Arrixaca, Murcia, Spain

[15]Paediatric Department, Osakidetza, Biocruces Bizkaia Health Research Institute, Hospital Universitario Cruces, Barakaldo, Spain

[16]Paediatric Department, Universidad del Pais Vasco UPV/EHU, Leioa, Spain

[17]Paediatric Oncology Department, Hospital La Fe, Valencia, Spain

[18]Anatomic Pathology Department, Hospital La Fe, Valencia, Spain

[19]Biocruces Bizkaia Health Research Institute, Department of Genetics, Physical Anthropology & Animal Physiology, Science and Technology Faculty, University of the Basque Country, UPV/EHU, Leioa, Spain

Abbreviations: ABD, absence of biallelic deletion; CN, copy number; CNA, copy number alteration; CNN-LOH, copy number neutral-loss of heterozygosity; EFS, event-free survival; FFPE, formalin-fixed paraffin embedded; FISH, fluorescence in situ hybridization; FT, frozen tissue; LOH, loss of heterozygosity; NGS, next-generation sequencing; NHL, non-Hodgkin lymphoma; OM-LZ, octapeptide motif-leucine-zipper; PCR, polymerase chain reaction; r/r, relapsed/refractory; RNA-seq, RNA sequencing; RT-PCR, real-time polymerase chain reaction; T-ALL, T-cell acute lymphoblastic leukaemia; TCR, T-cell receptor; T-LBL, T-cell lymphoblastic lymphoma; TRG, T-cell receptor gamma.

[#]Julia Salmerón-Villalobos and Joan Enric Ramis-Zaldivar contributed equally to this work.
[*]Idoia Martin-Guerrero and Itziar Salaverria contributed equally to this work.

This is an open access article under the terms of the Creative Commons Attribution-NonCommercial-NoDerivs License, which permits use and distribution in any medium, provided the original work is properly cited, the use is non-commercial and no modifications or adaptations are made.
© 2022 The Authors. *Pediatric Blood & Cancer* published by Wiley Periodicals LLC.

15455017, 2022, 11, Downloaded from https://onlinelibrary.wiley.com/doi/10.1002/pbc.29926 by Universidad Del Pais Vasco, Wiley Online Library on [09/11/2022]. See the Terms and Conditions (https://onlinelibrary.wiley.com/terms-and-conditions) on Wiley Online Library for rules of use; OA articles are governed by the applicable Creative Commons License

Correspondence
Itziar Salaverria, Institut d'Investigacions Biomèdiques August Pi i Sunyer IDIBAPS, Rosselló 149–153, 08036-Barcelona, Spain.
Email: isalaver@clinic.cat

Abstract

Background: T-cell lymphoblastic lymphoma (T-LBL) is an aggressive neoplasm closely related to T-cell acute lymphoblastic leukaemia (T-ALL). Despite their similarities, and contrary to T-ALL, studies on paediatric T-LBL are scarce and, therefore, its molecular landscape has not yet been fully elucidated. Thus, the aims of this study were to characterize the genetic and molecular heterogeneity of paediatric T-LBL and to evaluate novel molecular markers differentiating this entity from T-ALL.

Procedure: Thirty-three paediatric T-LBL patients were analyzed using an integrated approach, including targeted next-generation sequencing, RNA-sequencing transcriptome analysis and copy-number arrays.

Results: Copy number and mutational analyses allowed the detection of recurrent homozygous deletions of 9p/*CDKN2A* (78%), trisomy 20 (19%) and gains of 17q24-q25 (16%), as well as frequent mutations of *NOTCH1* (62%), followed by the *BCL11B* (23%), *WT1* (19%) and *FBXW7*, *PHF6* and *RPL10* genes (15%, respectively). This genetic profile did not differ from that described in T-ALL in terms of mutation incidence and global genomic complexity level, but unveiled virtually exclusive 17q25 gains and trisomy 20 in T-LBL. Additionally, we identified novel gene fusions in paediatric T-LBL, including *NOTCH1–IKZF2*, *RNGTT–SNAP91* and *DDX3X–MLLT10*, the last being the only one previously described in T-ALL. Moreover, clinical correlations highlighted the presence of Notch pathway alterations as a factor related to favourable outcome.

Conclusions: In summary, the genomic landscape of paediatric T-LBL is similar to that observed in T-ALL, and Notch signaling pathway deregulation remains the cornerstone in its pathogenesis, including not only mutations but fusion genes targeting *NOTCH1*.

KEYWORDS
molecular genetics, Notch, paediatric, T-cell lymphoblastic lymphoma, T-LBL

1 | INTRODUCTION

Non-Hodgkin lymphoma (NHL) represents the fourth most frequent malignancy in children and adolescents. Among the different NHL entities, T-cell lymphoblastic lymphoma (T-LBL) accounts for 20% of cases and shares biological, clinical and therapeutic features with T-cell acute lymphoblastic leukaemia (T-ALL).[1,2] Although considered the same disease, it is still unclear if the different presentations are associated with biological differences.[3] However, studies exploring the molecular landscape of paediatric T-LBL are scarce in comparison to T-ALL.

Paediatric T-LBL presents a heterogeneous copy number (CN) profile, being loss of 9p21.3, targeting *CDKN2A* gene, the most recurrent copy number alteration (CNA) (25%–90%), as in T-ALL.[4–7] Regarding the mutational profile, paediatric T-LBL is characterized by frequent mutations of *NOTCH1*, *FBXW7*, *PTEN*, *STAT5B* and *BCL11B* genes. These alterations, similarly to T-ALL, affect Notch, PI3K/AKT and JAK/STAT signaling pathways and epigenetic modifiers.[6,8–11]

Survival of LBL has improved over the last decades (event-free survival [EFS] rates: 80%–90%),[12,13] but there is no salvage strategy stablished for relapsed/refractory (r/r) patients so far.[14] Therefore, the identification of biological prognostic factors is required for the design of individualized therapy strategies in high-risk and/or r/r cases. Retrospective molecular studies in T-LBL have shown some markers with prognostic impact: *NOTCH1* and *FBXW7* mutations (favourable),[8,15,16] 6q loss of heterozygosity (LOH),[8,17,18] mutations targeting the tumour suppressor *PTEN*, absence of biallelic deletion (ABD) of T-cell receptor (*TCR*) gamma (*TRG*) at chr7p14.1 locus and mutations in *KMT2D* (unfavourable).[6,10,15,19]

Cytogenetic and RNA-sequencing (RNA-seq) studies in paediatric and young adult T-ALL have identified recurrent driving rearrangements and fusion genes involving *TCR* genes and oncogenes, such as *HOXA*, *TLX1/3*, *NKX2-1/2-2*, *TAL1/2*, *LYL1*, *LMO1/2/3*, *MLLT10*, *KMT2A*.[11,20,21] Those rearrangements have also been identified by karyotype in paediatric T-LBL,[22] with higher incidence of t(9;17)(q34;q22-23) involving *NOTCH1* gene, in comparison with T-ALL.[23,24]

Moreover, transcriptome analysis of nine adult T-LBL has identified *NFYG–TAL1*, *RIC3–TCRBC2*, *SLC35A3–HIAT1* and *PICALM–MLLT10* as possible pathogenic gene fusions.[25] Differently, no RNA-seq has yet

15455017, 2022, 11, Downloaded from https://onlinelibrary.wiley.com/doi/10.1002/pbc.29926 by Universidad Del Pais Vasco, Wiley Online Library on [09/11/2022]. See the Terms and Conditions (https://onlinelibrary.wiley.com/terms-and-conditions) on Wiley Online Library for rules of use; OA articles are governed by the applicable Creative Commons License

TABLE 1 Clinical characteristics of 32 paediatric T-LBL patients with primary tumour samples and one additional case with only relapse sample available

Gender	*n* = 33	%
Male	26	78.8
Female	7	21.2
Age (years)		
Median (range)	11 (1–16)	
<10	15	45.5
10–14	14	42.4
≥15	4	12.1
General condition (Lansky)	32	
Good (80%–100%)	28	84.8
Intermediate (50%–70%)	4	12.1
Poor (≤40%)	0	
LDH		
<2× UNL	15	45.5
≥2× UNL	18	55.5
Stage (St. Jude)		
Stage I/II	0	
Stage III	25	75.8
Stage IV	8	24.2
BM involvement[a]		
Yes	5	15.2
No	28	84.8
CNS involvement		
Yes	3	9.1
No	30	90.9
Nodal presentation	33	100
Extranodal presentation	13	39.4
Pleural effusion	9	69.2
Other	4	30.8
Events		
Relapse	9	27.3
Exitus	9	27.3
Second malignancy	0	
Relapse (*n* = 9)		
Local	3	33.3
BM	2	22.2
CNS	2	22.2
Combined	2	22.2
Time from diagnosis to relapse (*n* = 9)		
Intra-treatment	8	88.9
Unknown	1	11.1
Median time (range) (months)	9 (2–15)	
Disease as cause of death (*n* = 9)	9	100

(Continues)

TABLE 1 (Continued)

Gender	*n* = 33	%
Time from relapse to exitus (months)		
Median (range)	5 (0–8)	
5-year EFS rate	71%	
5-year OS rate	71%	

Abbreviations: BM, bone marrow; CNS, central nervous system; EFS, event-free survival; LDH, lactate dehydrogenase; OS, overall survival; UNL, upper normal limit.

[a]BM involvement was defined by ≥5% blasts in aspiration smears.

been performed in paediatric T-LBL for the identification of additional cryptic structural variants.

The present study aims to molecularly characterize a paediatric series of T-LBL using different next-generation sequencing (NGS) techniques, to elucidate the relevance of the current known and novel prognostic markers and to evaluate novel molecular markers differentiating this entity from T-ALL.

2 | METHODS

2.1 | Patients and samples

Thirty-three paediatric patients (<18 years) with T-LBL diagnosis, included in the national NHL registry of the Sociedad Española de Hematología y Oncología Pediátricas (SEHOP), and with biological material available for research, were retrospectively selected (diagnosed between 2002 and 2020). All samples were centrally reviewed by two hematopathologists (Olga Balagué and Blanca Gonzalez-Farré). All patients showed a bone marrow involvement inferior to 25% according to the internationally accepted definition for LBL versus ALL.[26] In two patients (cases #12 and #17), both primary tumour and relapse were collected and case #38R was included with only sample at relapse.

Twenty-six out of the 33 patients were male (78.8%) and 29 cases (87.9%) were younger than 15 years old at diagnosis. All patients presented an advanced disease according to St. Jude classification (stage III: 75.8%; stage IV: 24.2%) (Table 1). Most patients (31/33, 93.9%) received first-line treatment according to local standards, in line to the Euro-LB02 strategy.[13]

This study was approved by the institutional review boards of collaborating institutions in accordance with the Declaration of Helsinki.

2.2 | Immunohistochemistry and clonality analysis

Immunohistochemistry analyses were performed using standard protocols. The morphology, growth pattern, cytology, and immunohistochemical stains were evaluated as part of the diagnostic workup

15455017, 2022, 11, Downloaded from https://onlinelibrary.wiley.com/doi/10.1002/pbc.29926 by Universidad Del Pais Vasco, Wiley Online Library on [09/11/2022]. See the Terms and Conditions (https://onlinelibrary.wiley.com/terms-and-conditions) on Wiley Online Library for rules of use; OA articles are governed by the applicable Creative Commons License

according to WHO criteria (Table S1).[26] *TRG* clonal rearrangement detection was performed using the polymerase chain reaction (PCR) BIOMED-2 protocols.[27] Selected cases were further analyzed for clonal rearrangements in the *TCR* beta gene using the BIOMED-2 protocol.[27]

2.3 | DNA copy number alterations analysis

CNA were examined in 35 samples (32 primary samples and three relapse samples) from 33 patients using Oncoscan CNV (12 samples) and Cytoscan (23 samples) platforms (ThermoFisher Scientific, Waltham, MA, USA) following standard protocols (Supporting Information; Figure S1). Gains and losses and CN neutral LOH (CNN-LOH) regions were evaluated using Nexus Biodiscovery v9.0 software (Biodiscovery, Hawthorne, CA, USA). Previously published paediatric T-ALL and T-LBL CN data were used for comparison.[4–6,28]

2.4 | Targeted NGS and mutational analysis

Twenty-six samples at diagnosis, 20 frozen tissue (FT) and six formalin-fixed paraffin-embedded (FFPE) tissue, and three samples at relapse (two FT and one FFPE) were available for interrogation of the mutational status of 43 T-cell lymphoma and leukaemia-related genes (Figure S1 and Table S2) using a SureSelectXT Target Enrichment System Capture NGS strategy library (Agilent Technologies, Santa Clara, CA, USA) before sequencing in a MiSeq equipment (Illumina, San Diego, CA, USA) (Supporting Information).

As no germline DNA was available and in order to select somatic variants, potential driver mutations were predicted according to previously published criteria[29] in which 90% of the mutations classified as functional were demonstrated to be somatic. Inclusion criteria were (a) variants described previously as somatic or functional on previous reports or COSMIC (v84); (b) all truncating variants (nonsense, frameshift, splice donor or acceptor mutations); and (c) the remaining missense variants that were predicted to be functionally deleterious using Mutation Assessor[30] or SIFT predictor[31] if a score was not provided by Mutation Assessor. Other functional predictors as Polyphen-2 (Polymorphism Phenotyping-2)[32] were also applied (Figure S2).

The contribution of each gene to previously defined pathways was investigated considering information extracted from either databases www.genecards.org and https://www.ncbi.nlm.nih.gov/gene/ or from previously published literature (Supporting Information; Table S2). Variant verification was performed on 19 cases using Nextera XT NGS method (Illumina, San Diego, CA, USA) (Figure S1 and Table S3), RNA-seq and Sanger sequencing (Table S4; Supporting Information). Previously published mutational profiles of paediatric T-ALL[11] and T-LBL[6] were used for comparisons.

2.5 | RNA-seq

Whole transcriptome analysis of nine T-LBL with high-quality RNA available (Figure S1) and three controls (T cells isolated from peripheral blood from non-cancer paediatric donors) was performed. RNA libraries were generated using TruSeq Stranded Total RNA Library Prep Kit and sequenced on the NovaSeq 6000 System (Illumina, San Diego, CA, USA) (Supporting Information). Gene expression analysis was performed with DESeq2 (R package). Variants were identified using VarScan and Haplotype Caller (GATK). Fusion genes variants were detected with the FusionCatcher software (Supporting Information).[33] Variant verifications were performed using real-time polymerase chain reaction (RT-PCR) (Table S4) and fluorescence in situ hybridization (FISH) on cryo slides (Supporting Information; Table S5).

2.6 | Statistical methods

Survival probabilities were estimated with the Kaplan–Meier method and differences assessed by the log-rank test for variables present in at least three cases. EFS was calculated as previously described.[34] Differences in the distribution of individual parameters among patient subsets were analyzed by Fisher's exact test for categorized variables, and the Student's *t*-test for continuous variables. Non-parametric tests were applied when necessary. The *p*-values for multiple comparisons were adjusted using the Benjamini–Hochberg correction false discovery rate (FDR). A cutoff of $p = .05$ was considered significant unless otherwise indicated. Statistical analyses were carried out using R software v3.5.0.

3 | RESULTS

3.1 | Clinicopathological characteristics

Morphological and immunohistochemical studies confirmed the diagnosis of T-LBL. In detail, all cases studied expressed CD3, CD5 and/or CD7. TdT expression was detected in 86.2% (25/29) of the samples. CD20 was negative in 92.8% (26/28), with two samples showing positivity in focal areas. Monoclonality for *TCR* gene rearrangements was demonstrated in 80% (24/30) (Table S1 and Figure S3).

Nine patients suffered relapse (27%) during treatment, with a median time from diagnosis to relapse of 9 months (range 2–15 months). Four patients presented central nervous system involvement in their relapse (two isolated and two combined with other locations), with a median time of relapse of 3 months (range 2–10 months). None of the relapsed patients survived despite different salvage approaches. The 5-year overall survival (OS) and EFS rates were 71% (Figure 1A).

15455017, 2022, 11, Downloaded from https://onlinelibrary.wiley.com/doi/10.1002/pbc.29926 by Universidad Del Pais Vasco, Wiley Online Library on [09/11/2022]. See the Terms and Conditions (https://onlinelibrary.wiley.com/terms-and-conditions) on Wiley Online Library for rules of use; OA articles are governed by the applicable Creative Commons License

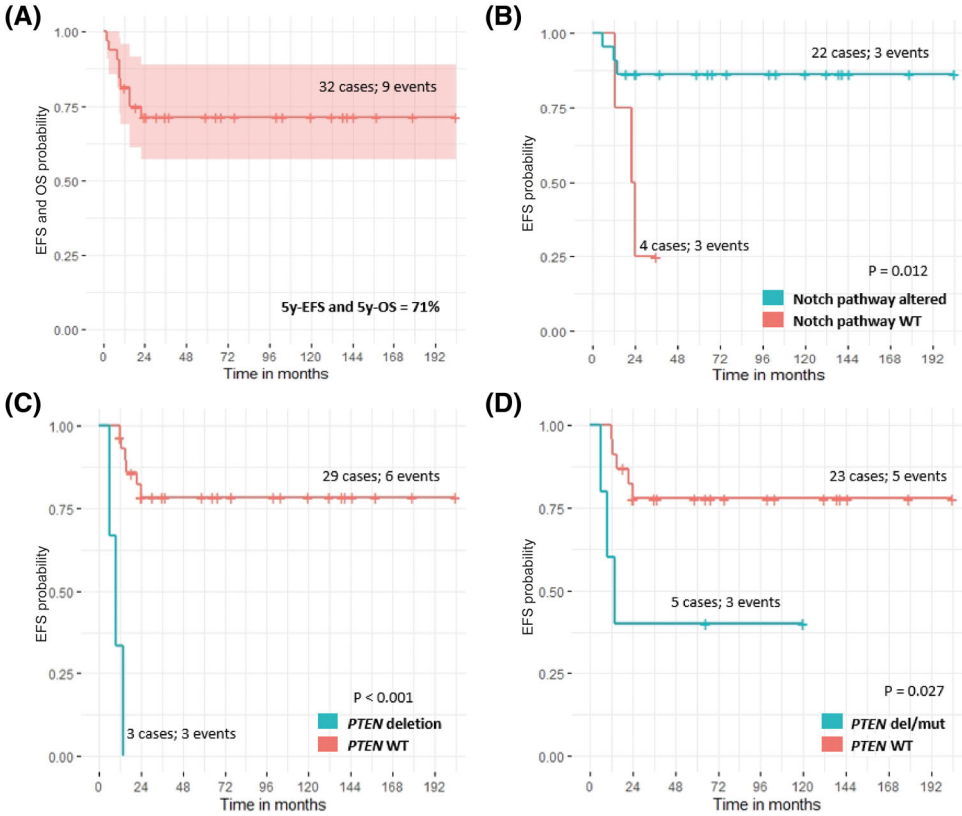

FIGURE 1 (A) Event-free survival (EFS) probability of 32 T-LBL patients for (B) Notch pathway alteration, (C) *PTEN* deletion and (D) *PTEN* alteration (either CN loss and/or mutation). EFS probability is represented in the vertical axis, while the horizontal axis depicts the time in months.

3.2 | Copy number profile

Copy number array analysis identified 188 CNA in all 32 primary tumour samples (5.8 alterations/case; range 1–41) (Table S6; Figure 2A). Recurrent alterations were losses of 9p21/*CDKN2A* in 25 out of 32 cases (78%), with 92% (23/25) showing homozygous deletions, mainly in the context of 9p CNN-LOH, followed by trisomy 20 in six cases and gains of 17q24-q25 in five cases. Two out of four cases with 17q gains showed concurrent 17p deletion, including *TP53* gene, suggestive of isochromosome 17. Of note, three cases displayed focal deletion of 10q23.31/*PTEN* locus, one of them with concomitant mutation of the gene.

Alterations associated with unfavourable prognosis as 6q deletions and ABD of the *TRG* locus were observed in two (both relapsed) and eight cases, respectively. Furthermore, two cases showed suggestive patterns of chromothripsis with recurrent alterations on chromosome 9 involving loss of first exons of *PTPRD* gene in both cases.

Paired sample analysis of diagnosis-relapse case #12 displayed acquisition of two genetic events at relapse (CNN-LOH in 1q21.2-1q44 and loss in 9p21.2-p21.1) (Figure S4A). Relapse sample of case #17 acquired five CNA (losses of 5q23.1-5q32, 12p13.31-12p13.1, 12q12, 15q21.3 and 15q24.3-q25.1) and had absence of two previously identified gains at 10p12.31-q26.3 and 11q14.2-q25 (Figure S4B). Additionally, CN analysis of case #38R, which had only relapse sample analyzed, showed 9p21.3-p21.2 homozygous deletion and several CNN-LOH regions (Table S6).

CN profile comparison of this T-LBL cohort with previously published CN data of T-ALL[28] showed no significant differences in global genomic complexity (6.6 in T-LBL vs. 3.5 alterations/case in T-ALL) (Figure 2B). Comparative analysis also revealed that losses of 9p21.3/*CDKN2A* were highly present in both diseases. Nevertheless, trisomy 20 and gains of 17q25 were virtually exclusive of T-LBL (22% vs. 0% and 16% vs. 5%, respectively; Fisher test p-adj < .05). Higher frequency of 6q16-q23 loss was also observed in T-ALL (6% vs. 17%), although not significant. However, due to the different resolution of both CN platforms (T-ALL were analyzed by Human Genome CGH 244A array), results must be taken cautiously.

3.3 | Identification of mutational profiles by targeted NGS

Targeted sequencing of 25 T-LBL at diagnosis, combined with mutational information obtained from RNA-seq of one case, identified a total of 84 variants in 24 cases. Of these variants, seventy-three (87%) were predicted as drivers (mean 2.8 alterations/case; range 1–5) (Figure 3). A verification rate of 100% of the selected variants was achieved with different techniques (Table S7). The most recurrently affected gene was *NOTCH1*, with 20 mutations (12 truncating

15455017, 2022, 11, Downloaded from https://onlinelibrary.wiley.com/doi/10.1002/pbc.29926 by Universidad Del Pais Vasco, Wiley Online Library on [09/11/2022]. See the Terms and Conditions (https://onlinelibrary.wiley.com/terms-and-conditions) on Wiley Online Library for rules of use; OA articles are governed by the applicable Creative Commons License

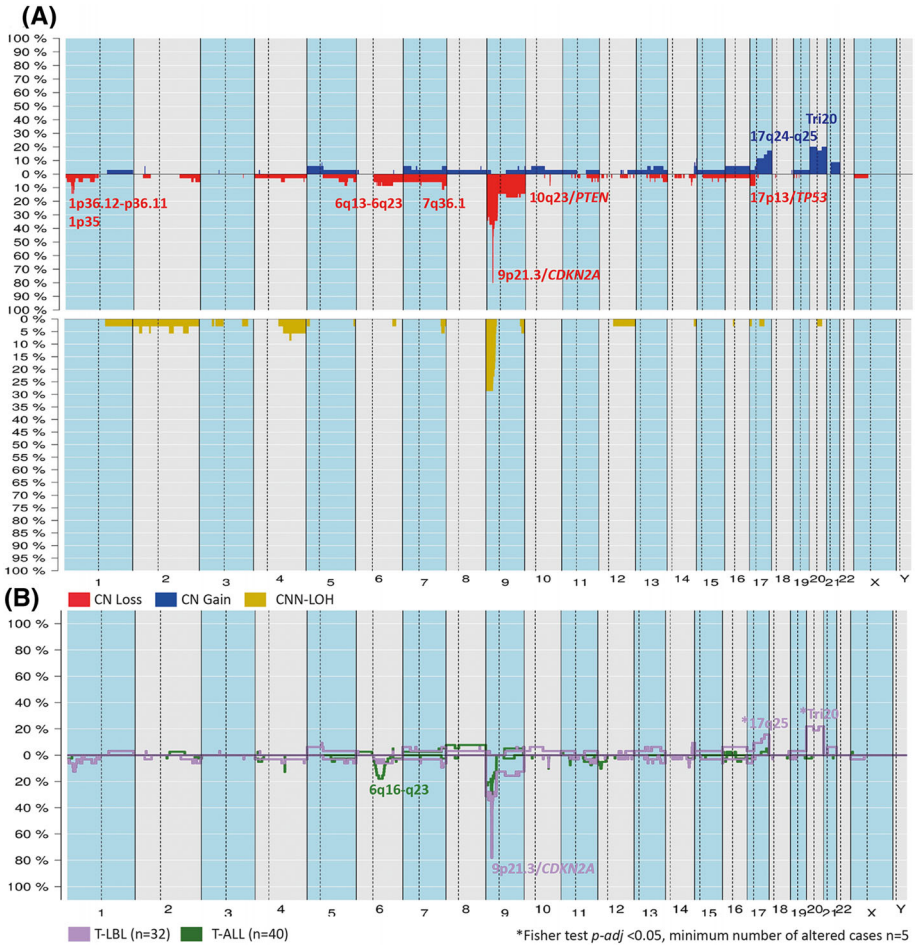

FIGURE 2 Copy number profile paediatric of T-LBL cases. (A) Global copy number profile of 32 T-LBL. The X-axis indicates chromosomes from 1 to Y and p to q. The vertical axis indicates frequency of each genomic aberration among the analyzed cases. Gains are depicted in blue while losses in red. Most frequently recurrent regions are indicated. (B) Comparative plot of copy number data between current series of 32 paediatric T-LBL and data from 40 T-ALL cases.[28] Purple colour identifies T-LBL, and green T-ALL cases. Asterisks indicate significant differences between both groups according to Fisher test *p*-adj < .05, considering a minimum number of altered cases $n = 5$.

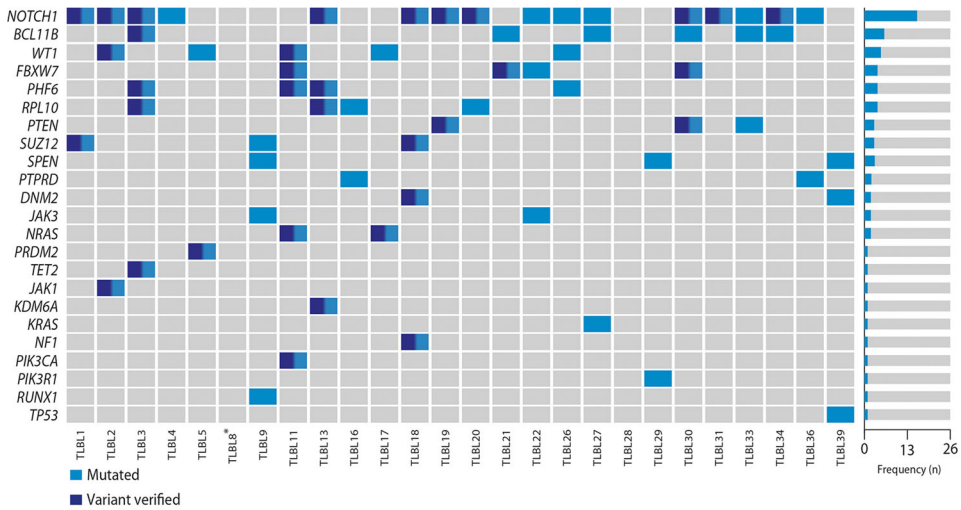

FIGURE 3 Mutational landscape of 26 paediatric T-LBL cases. The figure depicts driver mutations identified in 26 pediatric T-LBL cases, with variants verified by Nextera XT technology or Sanger sequencing represented in dark blue, whereas grey represents absence of mutation. Asterisk marks case with mutational information obtained from RNA-seq data.

15455017, 2022, 11, Downloaded from https://onlinelibrary.wiley.com/doi/10.1002/pbc.29926 by Universidad Del Pais Vasco, Wiley Online Library on [09/11/2022]. See the Terms and Conditions (https://onlinelibrary.wiley.com/terms-and-conditions) on Wiley Online Library for rules of use; OA articles are governed by the applicable Creative Commons License

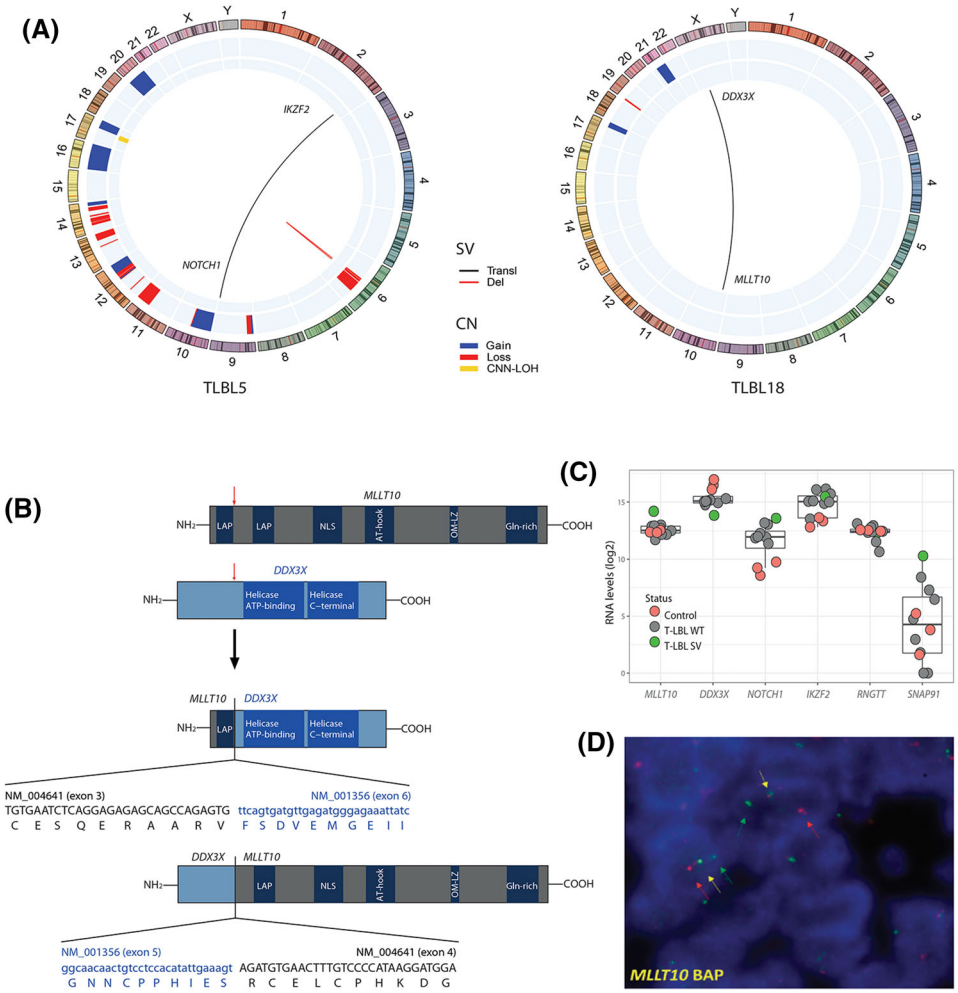

FIGURE 4 Fusion genes in two T-LBL cases detected from RNA-seq. (A) Circos plot of cases TLBL5 and TLBL18 including fusion genes detected by RNA-seq (lines) and CN alterations (outer circle) and copy number neutral-loss of heterozygosity (CNN-LOH) (inner circle) detected by CN arrays. CN colours indicate gains (blue), losses (red) and CNN-LOH (yellow). (B) Schematic representation of *DDX3X–MLLT10* fusion breakpoints and putative fusion protein structure in TLBL18. GenBank accession numbers are indicated for both genes. (C) Gene expression levels by RNA-seq of the fused genes. Y-axis represents log2 levels. Pink dots represent T-cell controls, green dots T-LBL cases with the fused gene and grey dots T-LBL without the rearrangement. Gln-rich: glutamine-enriched domain; LAP: leukaemia-associated protein; NLS: nuclear localization signal; OM-LZ: octapeptide motif-leucine-zipper; wt: wild-type. (D) FISH showed separated green and red signals in TLBL18, indicating a *MLLT10* break (arrows).

clustering within the PEST domain and eight missense grouped in the HD domain) in 16 (62%) cases. Second most mutated gene was *BCL11B*, with seven mutations (five truncating and two missense) in six (23%) cases, and variants clustering in the zinc finger structures coded by the exon 4 of the gene. Comparison of the mutational profile of these 26 T-LBL with previously published data on 121 paediatric T-LBL[6] and 264 paediatric T-ALL[11] showed similar mutational profiles with no significant differences (Table S8).

Interestingly, paired primary tumour relapse (#17) showed retention of the mutations present in the diagnosis sample, affecting *NRAS* and *WT1* genes (Figure S4C), and one additional mutation in *PAPPA*. Additionally, relapsed sample from case #12R harboured mutations in *FLT3* and *TP53*. Mutations in *PIK3R1* and *PTPN2* were detected in case #38R.

3.4 | Fusion transcript discovery

RNA-seq transcriptome data on nine paediatric T-LBL primary samples were investigated for the presence of fusion transcripts rendering nine fusion genes. After applying stringent inclusion and exclusion criteria (Supporting Information), three high-confidence fusion transcripts in two patients were considered *bonafide* variants and were verified using ortholog techniques detailed in Table S9. In case #5, two fusion genes were detected, including *NOTCH1–IKZF2*, resulting from rearrangement t(2;9)(q34;q34.3), and *RNGTT–SNAP91*, as a product of a 6q14.2-q15 deletion. In case #18, a reciprocal translocation t(10;X)(p12.31;p11.4), leading to *DDX3X–MLLT10* fusion gene, was identified (Figure 4A). In detail, *NOTCH1–IKZF2* fusion transcript binds *IKZF2* exon 6 to *NOTCH1* exon 27, resulting in a chimeric protein

15455017, 2022, 11, Downloaded from https://onlinelibrary.wiley.com/doi/10.1002/pbc.29926 by Universidad Del Pais Vasco, Wiley Online Library on [09/11/2022]. See the Terms and Conditions (https://onlinelibrary.wiley.com/terms-and-conditions) on Wiley Online Library for rules of use; OA articles are governed by the applicable Creative Commons License

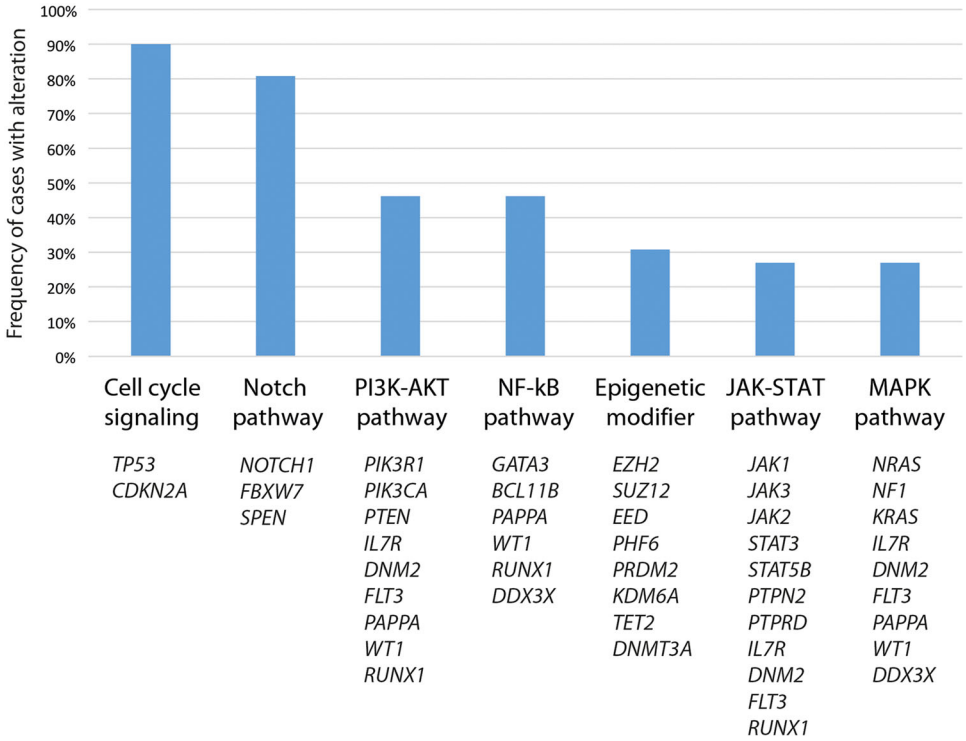

FIGURE 5 Pathway enrichment analysis. The frequency of cases presenting alteration of each pathway is represented in the vertical axis. Contribution of each gene to previously defined pathways has been assigned according to either databases www.genecards.org and https://www.ncbi.nlm.nih.gov/gene or to previously published literature (Table S2).[45–74]

containing the DNA-binding domains of *IKZF2* and the transmembrane and intracellular subunit of *NOTCH1*, which acts as a transcription factor. RNA-seq expression data confirmed similar levels of *NOTCH1* expression than in the *NOTCH1* mutated cases (Figure S5). *IKZF2* expression levels of the case with the translocation were like those detected in cases without it (Figure 4C). We also detected *RNGTT–SNAP91* fusion gene, where *SNAP91* exon 12 was juxtaposed to *RNGTT* exon 13, resulting in a deletion of 6q14.2-q15. Case #5 presented expression levels of *RNGTT* in line with cases lacking this rearrangement, whereas *SNAP91* expression was higher than in those cases without the translocation (Figure 4C).

Finally, *DDX3X–MLLT10* rearrangement fused *DDX3X* exon 6 to *MLLT10* exon 4, as previously described in paediatric and adult T-ALL.[11,35,36] This structural variant produces a fusion transcript that retains the *MLLT10* octapeptide motif-leucine-zipper (OM-LZ) domain (Figure 4B). This fusion gene led to an overexpression of *MLLT10* and downregulation of *DDX3X* according to RNA-seq expression data (Figure 4C). This alteration was verified using *MLLT10* break-apart probe (Figure 4D) and RT-PCR.

3.5 | Pathway enrichment analysis on paediatric T-LBL

To identify possible enrichments of key pathways, CN and NGS data of 26 paediatric T-LBL were integrated. The analysis showed that all cases were affected by genes involved in cell cycle signaling (*TP53* and *CDKN2A* losses) (27/30 cases, 90%) and/or Notch pathway (*NOTCH1*, *FBXW7* and *SPEN* mutations) (23/26 cases each, 88%) (Figure 5).

Additionally, we performed differential expression analysis of transcriptomic data and identified 3583 out of 17,805 protein-coding genes (15%) differentially expressed, from which 2480 were upregulated and 1103 downregulated in the T-LBL group (p-adj < .01; log2 fold change $\geq 2/\leq -2$). Pathway enrichment analysis of these differentially expressed genes showed enrichment in genes related to cell communication (GO:0007154; q-value = 1.65E-45), and cell migration (GO:0016477; q-value = 1.83E-40), in addition to previously mentioned cell cycle signaling (GO:0007049; q-value = 0.0046) and Notch signaling pathway (GO:0007219; q-value = 0.0025), among others (Table S10).

3.6 | Prognostic correlations

Prognostic correlations were performed on clinical and recurrent genetic alterations. These analyses revealed that only alterations of genes involved in Notch pathway were significantly associated with favourable outcome (5-year EFS 86% vs. 25%; $p = .012$) (Figure 1B) and *PTEN* alterations (loss and/or mutation) associated with unfavourable outcome (5-year EFS 40% vs. 78%; $p = .027$) (Figure 1C,D). This same tendency towards a worse clinical outcome was observed in relation to previously published markers such as high LDH levels (5-year EFS 73% vs. 100%; $p = .35$) and ABD of *TRG* (5-year EFS 52% vs. 78%; $p = .13$).

15455017, 2022, 11, Downloaded from https://onlinelibrary.wiley.com/doi/10.1002/pbc.29926 by Universidad Del Pais Vasco, Wiley Online Library on [09/11/2022]. See the Terms and Conditions (https://onlinelibrary.wiley.com/terms-and-conditions) on Wiley Online Library for rules of use; OA articles are governed by the applicable Creative Commons License

4 | DISCUSSION

The genetic landscape of paediatric T-LBL has been poorly investigated, and differences and similarities with the leukaemic counterpart T-ALL have not been well defined. In the present study, we have performed a high-resolution analysis of the genomic landscape of 33 paediatric T-LBL, combining for the first time data derived from CN study, mutational and gene expression profiling.

The genetic profile observed showed genetic alterations mainly affecting cell cycle genes, Notch and JAK/STAT signaling pathways and epigenetic modifiers including loss of 9p21.3 targeting *CDKN2A* gene and frequent mutations of *NOTCH1*, *BCL11B*, *WT1*, *FBXW7*, *PHF6* and *RPL10* genes. In terms of CN, paediatric T-LBL displayed a CN profile similar to T-ALL[28] but with higher incidence of trisomy 20 and CN gains of 17q.25. Our data are also in line with previously published CN data on paediatric T-LBL series (Figure S6),[4–6] although we could not identify 13q14.2 deletions as described in previous studies.[5,7] Interestingly, we observed chromothripsis-like patterns in two cases affecting chromosome 9. Both patients presented alteration of the cell cycle signaling due to 9p21/*CDKN2A* deletion, JAK/STAT pathway, because of 9p24.1-p23/*PTPRD* loss, and mutations in epigenetic modifiers. The *PTPRD* gene encodes the receptor-type-protein-tyrosine-phosphatase-*δ*, a tumour suppressor gene that, in addition to *CDKN2A*, is involved in cell growth regulation, which has been described to be frequently mutated in nodal marginal zone lymphoma, among other cancers.[37]

Regarding the mutational landscape, comparison with 264 paediatric T-ALL[11] showed similar mutational profiles in which most of the identified mutations could be assigned to Notch, PI3K/AKT and JAK/STAT signaling pathways and epigenetic modifiers. These results were in line with previously analyzed series of 121 paediatric and adolescent T-LBL[6] (Table S8), with *NOTCH1* being the most recurrently mutated gene in both sets. However, we were not able to identify previously reported *KMT2D* poor prognostic mutations in any of the nine cases analyzed by RNA-seq nor *PIK3CA* mutations associated to relapse, probably due to the limited number of cases analyzed.[6,38]

Globally, integration of mutational information with CN results revealed cell cycle and Notch signaling as the main oncogenic pathways in T-LBL, as previously reported.[6] Gene expression pathway enrichment analysis also showed cell cycle and Notch signaling overrepresented in our series, reinforcing the importance of these pathways in the disease. This genomic landscape matches with that described in T-ALL.[39]

Interestingly, in paired tumour-relapse samples, we observed that relapse samples were more complex that diagnosis due to the acquisition of genetic alterations and lack of specific recurrent alterations.

Our RNA-seq data analysis identified three *bonafide* fusion genes not described so far in paediatric T-LBL patients. We detected *DDX3X–MLLT10* fusion, which has been reported in paediatric T-ALL cases[36] and approximately 3% of adult T-ALL, characterizing a subgroup of *NOTCH1*-positive leukaemias.[35] This fusion has been described to retain *MLLT10* OM-LZ domain, necessary to induce leukaemia.[40] Despite the low number of our cases, RNA-seq expression data confirmed higher expression of the fused *MLLT10* in comparison to additional T-LBL and T-cell controls analyzed (Figure 4C). Of note, *MLLT10* gene has been reported to be translocated with other partners in paediatric and young adult T-ALL[11] and adult T-LBL,[25] and has been associated with upregulation and overexpression of homeobox A (*HOXA*) genes.[35,41] In line with these reports, the case with *DDX3X–MLLT10* fusion presented higher HOXA9 expression levels in comparison with T-cell controls and T-LBL cases without the rearrangement. Additionally, two novel fusion genes not previously reported in T-LBL/ALL could be identified for the first time. *NOTCH1–IKZF2* translocation fused *IKZF2* exon 6 to *NOTCH1* exon 27. As a result, *NOTCH1* losses its C-terminal PEST domain which, similarly to activating mutations altering this region, interferes with ubiquitination-mediated downregulation and leads to prolonged half-life of intracellular NOTCH1 fragment. In fact, RNA-seq expression data confirmed similar expression levels of the fused *NOTCH1* when compared to the rest of cases affected by other Notch pathway alterations (Figure S5). Therefore, this fusion gene could act as an alternative activation mechanism of the Notch pathway. Interestingly, different rearrangements of the 9q34/*NOTCH1* locus have been reported in ∼10% of paediatric T-LBL patients.[23,24] Besides, *IZKF2*, a chromatin remodeler highly expressed in leukaemic stem cells, has been described to be mutated in 2% of T-ALL and translocated with *BCL11B* in the context of the t(2;14)(q34;q32)/*IKZF2-BCL11B* rearrangement.[11,42] The other fusion gene observed was *RNGTT–SNAP91*. The significance of this fusion is uncertain, although it led to 6q14.2-q15 deletion, an alteration frequently observed in lymphomas[29,43,44] and associated with bad prognosis in T-LBL.[8,17,18] Interestingly, patient carrying this fusion relapsed 8 months after diagnosis and eventually deceased in the following 5 months.

In our study, EFS was inferior than the one described in the European Intergroup Euro-LB02 trial (71% vs. 82%).[13] This difference could be explained by the retrospective nature of our study and the low number of patients included. However, survival analyses confirmed the importance of Notch pathway alterations as favourable prognostic markers.[8,15,16] Interestingly, alterations of tumour suppressor gene *PTEN*, including deletions and mutations, were associated with poor prognosis. Differently to previous studies where mutations alone of the gene have been associated with worse prognosis,[10,19] only mutations did not confer any different outcome in our T-LBL series. The prognostic impact of 6q LOH could not be demonstrated due to the low number of cases with this alteration, but the two identified cases with this alteration relapsed, suggesting its association with an unfavourable outcome.[8,17,18] On the other hand, ABD associations with worse prognosis could not be demonstrated, although a tendency was observed.[15]

Our integrative approach including morphological, CN and NGS sequencing analyses in a large series of paediatric T-LBL confirms that this disease is genetically heterogeneous, with *CDKN2A* deletions and *NOTCH1* mutations as the most recurrent genetic features, with high degree of genomic complexity including chromothripsis-like patterns and presence of novel fusion transcripts. Globally, our results reinforce the implication of key pathways like cell cycle

15455017, 2022, 11, Downloaded from https://onlinelibrary.wiley.com/doi/10.1002/pbc.29926 by Universidad Del Pais Vasco, Wiley Online Library on [09/11/2022]. See the Terms and Conditions (https://onlinelibrary.wiley.com/terms-and-conditions) on Wiley Online Library for rules of use; OA articles are governed by the applicable Creative Commons License

regulation and Notch signaling in the pathogenesis of the disease and highlight its similarities with T-ALL. These insights into T-LBL biology should contribute to future drug development strategies in relapsed-refractory patients with currently unsatisfactory salvage options.

ACKNOWLEDGMENTS

We thank the centres of the Sociedad Española de Hematología y Oncología Pediátricas that submitted cases for consultation, to Noelia Garcia, Silvia Martín and Helena Suarez for their excellent technical assistance and to Nerea Dominguez for updating clinical data. We are indebted to the IDIBAPS Genomics Core Facility and to the HCB-IDIBAPS, the Hospital Infantil Sant Joan de Déu and the Hospital Universitari *Vall d'Hebron* Tumour Biobanks, all integrated in the National Network Biobanks of ISCIII for the sample and data procurement. This work was supported by Asociación Española Contra el Cáncer (AECC CICPFI6025SALA and 'Ayudas Clínico Formación AECC 2020' to Jaime Verdú-Amorós), Asociación de aitas y amas para la humanización, socialización e investigación del Cáncer Infantil y la divulgación de la donación de medula ósea-La Cuadri del Hospi, Fondo de Investigaciones Sanitarias Instituto de Salud Carlos III (Miguel Servet Program I and II CP13/00159 and MSII18/00015; Itziar Salaverria), Generalitat de Catalunya Suport Grups de Recerca (2017-SGR-1107; Itziar Salaverria), and the European Regional Development Fund 'Una manera de fer Europa'. Joan Enric Ramis-Zaldivar was supported by a fellowship AGAUR FI-DGR 2017 (2017 FI_B01004) from Generalitat de Catalunya. Noelia Garcia has been continuously supported by Acció instrumental d'incorporació de científics i tecnòlegs PERIS 2016 (SLT002/16/00336) and PERIS 2020 (SL017/20/000204) from Generalitat de Catalunya. Julia Salmerón-Villalobos was supported by a fellowship from La Caixa (CLLEvolution-HR17-00221). This work was developed partially at the Centro Esther Koplowitz, Barcelona, Spain.

CONFLICT OF INTEREST

The authors declare they have no conflicts of interest.

AUTHOR CONTRIBUTIONS

Julia Salmerón-Villalobos and Joan Enric Ramis-Zaldivar performed research, analyzed data and wrote the manuscript. Olga Balagué performed centralized morphological diagnosis and analyzed data. Sara Mato, Angela Gutierrez-Camino, Daniel Sinnett, Unai Illarregi, Máxime Carron, Noelia Garcia and Dolors Colomer performed research and analyzed data. Blanca Gonzalez-Farré, Marta Garrido, Elias Campo and Margarita Llavador reviewed and interpreted pathological data. Jaime Verdú-Amorós, Verónica Celis, Constantino Sábado, Javier Uriz, M. José Ortega, Alexandra Regueiro, Ana Galera, Itziar Astigarraga and Mara Andrés reviewed and interpreted clinical data. Itziar Salaverria and Idoia Martin-Guerrero performed research, analyzed data, designed research and wrote the manuscript. All authors approved the final version of the manuscript.

DATA AVAILABILITY STATEMENT

Sequencing data have been deposited at the European Nucleotide Archive (ENA, accession number ERP127734). The copy number and gene expression data reported in this article have been deposited at GEO database under accession number GSE178427.

ORCID

Julia Salmerón-Villalobos https://orcid.org/0000-0002-7092-9160
Joan Enric Ramis-Zaldivar https://orcid.org/0000-0001-7108-7738
Olga Balagué https://orcid.org/0000-0002-5099-3675
Jaime Verdú-Amorós https://orcid.org/0000-0002-0900-0889
Constantino Sábado https://orcid.org/0000-0003-3956-5466
Sara Mato https://orcid.org/0000-0001-7269-2470
Angela Gutierrez-Camino https://orcid.org/0000-0002-8679-6868
Daniel Sinnett https://orcid.org/0000-0003-3625-6676
Unai Illarregi https://orcid.org/0000-0001-7418-5616
Máxime Carron https://orcid.org/0000-0002-3733-5723
Alexandra Regueiro https://orcid.org/0000-0003-3156-4784
Ana Galera https://orcid.org/0000-0002-5355-8003
Blanca Gonzalez-Farré https://orcid.org/0000-0002-1796-7248
Elias Campo https://orcid.org/0000-0001-9850-9793
Dolors Colomer https://orcid.org/0000-0001-7486-8484
Itziar Astigarraga https://orcid.org/0000-0002-5012-0137
Mara Andrés https://orcid.org/0000-0001-8274-5724
Idoia Martin-Guerrero https://orcid.org/0000-0002-0098-1908
Itziar Salaverria https://orcid.org/0000-0002-2427-9822

REFERENCES

1. SEER*Explorer: an interactive website for SEER cancer statistics [Internet]. Surveillance Research Program. National Cancer Institute. Accessed September 27, 2021. https://seer.cancer.gov/explorer/
2. Burkhardt B, Zimmermann M, Oschlies I, et al. The impact of age and gender on biology, clinical features and treatment outcome of non-Hodgkin lymphoma in childhood and adolescence. *Br J Haematol*. 2005;131(1):39-49.
3. Kroeze E, Loeffen JLC, Poort VM, Meijerink JPP. T-cell lymphoblastic lymphoma and leukemia: different diseases from a common premalignant progenitor? *Blood Adv*. 2020;4(14):3466-3473.
4. Basso K, Mussolin L, Lettieri A, et al. T-cell lymphoblastic lymphoma shows differences and similarities with T-cell acute lymphoblastic leukemia by genomic and gene expression analyses. *Genes Chromosom Cancer*. 2011;50(12):1063-1075.
5. Schraders M, van Reijmersdal SV, Kamping EJ, et al. High-resolution genomic profiling of pediatric lymphoblastic lymphomas reveals subtle differences with pediatric acute lymphoblastic leukemias in the B-lineage. *Cancer Genet Cytogenet*. 2009;191(1):27-33.
6. Khanam T, Seggewiss J, Ruether C, Zimmermann M, Mueller S, Burkhardt B. Integrative genomic analysis of pediatric T-cell lymphoblastic lymphoma reveals candidates of clinical significance. *Blood*. 2021;137(17):2347-2359.
7. Haider Z, Landfors M, Golovleva I, et al. DNA methylation and copy number variation profiling of T-cell lymphoblastic leukemia and lymphoma. *Blood Cancer J*. 2020;10(4):45.
8. Bonn BR, Rohde M, Zimmermann M, et al. Incidence and prognostic relevance of genetic variations in T-cell lymphoblastic lymphoma in childhood and adolescence. *Blood*. 2013;121(16):3153-3160.

15455017, 2022, 11, Downloaded from https://onlinelibrary.wiley.com/doi/10.1002/pbc.29926 by Universidad Del Pais Vasco, Wiley Online Library on [09/11/2022]. See the Terms and Conditions (https://onlinelibrary.wiley.com/terms-and-conditions) on Wiley Online Library for rules of use; OA articles are governed by the applicable Creative Commons License

9. Chang YH, Yu CH, Jou ST, et al. Targeted sequencing to identify genetic alterations and prognostic markers in pediatric T-cell acute lymphoblastic leukemia. *Sci Rep*. 2021;11(1):769.
10. Bonn BR, Huge A, Rohde M, et al. Whole exome sequencing hints at a unique mutational profile of paediatric T-cell lymphoblastic lymphoma. *Br J Haematol*. 2015;168(2):308-313.
11. Liu Y, Easton J, Shao Y, et al. The genomic landscape of pediatric and young adult T-lineage acute lymphoblastic leukemia. *Nat Genet*. 2017;49(8):1211-1218.
12. Reiter A, Schrappe M, Ludwig WD, et al. Intensive ALL-type therapy without local radiotherapy provides a 90% event-free survival for children with T-cell lymphoblastic lymphoma: a BFM group report. *Blood*. 2000;95(2):416-421.
13. Landmann E, Burkhardt B, Zimmermann M, et al. Results and conclusions of the European intergroup EURO-LB02 trial in children and adolescents with lymphoblastic lymphoma. *Haematologica*. 2017;102(12):2086-2096.
14. Burkhardt B, Reiter A, Landmann E, et al. Poor outcome for children and adolescents with progressive disease or relapse of lymphoblastic lymphoma: A report from the Berlin-Frankfurt-Muenster group. *J Clin Oncol*. 2009;27(20):3363-3369.
15. Callens C, Baleydier F, Lengline E, et al. Clinical impact of NOTCH1 and/or FBXW7 mutations, FLASH deletion, and TCR status in pediatric T-cell lymphoblastic lymphoma. *J Clin Oncol*. 2012;30(16):1966-1973.
16. Park MJ, Taki T, Oda M, et al. FBXW7 and NOTCH1 mutations in childhood T cell acute lymphoblastic leukaemia and T cell non-Hodgkin lymphoma. *Br J Haematol*. 2009;145(2):198-206.
17. Burkhardt B, Bruch J, Zimmermann M, et al. Loss of heterozygosity on chromosome 6q14-q24 is associated with poor outcome in children and adolescents with T-cell lymphoblastic lymphoma. *Leukemia*. 2006;20(8):1422-1429.
18. Burkhardt B, Moericke A, Klapper W, et al. Pediatric precursor T lymphoblastic leukemia and lymphoblastic lymphoma: Differences in the common regions with loss of heterozygosity at chromosome 6q and their prognostic impact. *Leuk Lymphoma*. 2008;49(3):451-461.
19. Balbach ST, Makarova O, Bonn BR, et al. Proposal of a genetic classifier for risk group stratification in pediatric T-cell lymphoblastic lymphoma reveals differences from adult T-cell lymphoblastic leukemia. *Leukemia*. 2016;30(4):970-973.
20. Ferrando AA, Neuberg DS, Staunton J, et al. Gene expression signatures define novel oncogenic pathways in T cell acute lymphoblastic leukemia. *Cancer Cell*. 2002;1(1):75-87.
21. Graux C, Cools J, Michaux L, Vandenberghe P, Hagemeijer A. Cytogenetics and molecular genetics of T-cell acute lymphoblastic leukemia: from thymocyte to lymphoblast. *Leukemia*. 2006;20(9):1496-1510.
22. Ellison DA, Parham DM, Sawyer JR. Cytogenetic findings in pediatric T-lymphoblastic lymphomas: one institution's experience and a review of the literature. *Pediatr Dev Pathol*. 2005;8(5):550-556.
23. Lones MA, Heerema NA, Le Beau MM, et al. Chromosome abnormalities in advanced stage lymphoblastic lymphoma of children and adolescents: a report from CCG-E08. *Cancer Genet Cytogenet*. 2007;172(1):1-11. https://doi.org/10.1016/j.cancergencyto.2006.07.011
24. Sekimizu M, Sunami S, Nakazawa A, et al. Chromosome abnormalities in advanced stage T-cell lymphoblastic lymphoma of children and adolescents: a report from Japanese Paediatric Leukaemia/Lymphoma Study Group (JPLSG) and review of the literature. *Br J Haematol*. 2011;154(5):612-617.
25. López-Nieva P, Fernández-Navarro P, Graña-Castro O, et al. Detection of novel fusion-transcripts by RNA-Seq in T-cell lymphoblastic lymphoma. *Sci Rep*. 2019;9(1):5179.
26. Swerdlow SH, Campo E, Harris NL, Jaffe ES, Pileri SA,Stein H, Thiele J, eds. *WHO Classification of Tumours of Haematopoietic and Lymphoid Tissues*. Revised 4th ed. IARC;2017.
27. Van Dongen J, Langerak AW, Brü Ggemann M, et al. Design and standardization of PCR primers and protocols for detection of clonal immunoglobulin and T-cell receptor gene recombinations in suspect lymphoproliferations: report of the BIOMED-2 Concerted Action BMH4-CT98-3936. *Leukemia*. 2003;17(12):2257-2317.
28. Gutierrez A, Sanda T, Grebliunaite R, et al. High frequency of PTEN, PI3K, and AKT abnormalities in T-cell acute lymphoblastic leukemia. *Blood*. 2009;114(3):647-650.
29. Karube K, Enjuanes A, Dlouhy I, et al. Integrating genomic alterations in diffuse large B-cell lymphoma identifies new relevant pathways and potential therapeutic targets. *Leukemia*. 2018;32(3):675-684.
30. Reva B, Antipin Y, Sander C. Predicting the functional impact of protein mutations: application to cancer genomics. *Nucleic Acids Res*. 2011;39(17):e118.
31. Kumar P, Henikoff S, Ng PC. Predicting the effects of coding non-synonymous variants on protein function using the SIFT algorithm. *Nat Protoc*. 2009;4(7):1073-1081.
32. Adzhubei IA, Schmidt S, Peshkin L, et al. A method and server for predicting damaging missense mutations. *Nat Methods*. 2010;7(4):248-249.
33. Nicorici D, Şatalan M, Edgren H, et al. FusionCatcher – a tool for finding somatic fusion genes in paired-end RNA-sequencing data. *bioRxiv*. 2014:11650. https://doi.org/10.1101/011650
34. Cheson BD, Pfistner B, Juweid ME, et al. Revised response criteria for malignant lymphoma. *J Clin Oncol*. 2007;25(5):579-586.
35. Brandimarte L, La Starza R, Gianfelici V, et al. DDX3X–MLLT10 fusion in adults with NOTCH1 positive T-cell acute lymphoblastic leukemia. *Haematologica*. 2014;99(5):64-66.
36. Brandimarte L, Pierini V, Di Giacomo D, et al. New MLLT10 gene recombinations in pediatric T-acute lymphoblastic leukemia. *Blood*. 2013;121(25):5064-5067.
37. Spina V, Khiabanian H, Messina M, et al. The genetics of nodal marginal zone lymphoma. *Blood*. 2016;128(10):1362-1373.
38. Ruether C, Wuensch C, Randau G, et al. Design of a targeted next-generation DNA sequencing panel for pediatric T-cell lymphoblastic lymphoma to unravel biology and optimize treatment. *Genes Chromosomes Cancer*. 2022;61(8):459-470.
39. Belver L, Ferrando A. The genetics and mechanisms of T cell acute lymphoblastic leukaemia. *Nat Rev Cancer*. 2016;16(8):494-507.
40. Deshpande AJ, Rouhi A, Lin Y, et al. The clathrin-binding domain of CALM and the OM-LZ domain of AF10 are sufficient to induce acute myeloid leukemia in mice. *Leukemia*. 2011;25(11):1718-1727.
41. Bond J, Bergon A, Durand A, et al. Cryptic XPO1-MLLT10 translocation is associated with HOXA locus deregulation in T-ALL. *Blood*. 2014;124(19):3023-3025.
42. Fujimoto R, Ozawa T, Itoyama T, Sadamori N, Kurosawa N, Isobe M. HELIOS–BCL11B fusion gene involvement in a t(2;14)(q34;q32) in an adult T-cell leukemia patient. *Cancer Genet*. 2012;205(7-8):356-364.
43. Chapuy B, Stewart C, Dunford A, et al. Molecular subtypes of diffuse large B-cell lymphoma are associated with distinct pathogenic mechanisms and outcomes. *Nat Med*. 2018;24(5):679-690.
44. Thelander EF, Ichimura K, Corcoran M, et al. Characterization of 6q deletions in mature B cell lymphomas and childhood acute lymphoblastic leukemia. *Leuk Lymphoma*. 2008;49(3):477-487.
45. Wang T, Lu Y, Polk A, et al. T-cell receptor signaling activates an ITK/NF-kB/GATA-3 axis in T-cell Lymphomas facilitating resistance to chemotherapy. *Clin Cancer Res*. 2017;23(10):2506-2515.
46. Li B, Chng WJ. EZH2 abnormalities in lymphoid malignancies : underlying mechanisms and therapeutic implications. *J Hematol Oncol*. 2019;12(1):118.
47. Cismasiu VB, Ghanta S, Duque J, et al. BCL11B participates in the activation of IL2 gene expression in CD4+ T lymphocytes. *Blood*. 2006;108(8):2695-2702.
48. Lau N, Feldkamp MM, Roncari L, et al. Loss of Neurofibromin Is Associated with Activation of RAS/MAPK and PI3-K/AKT

15455017, 2022, 11, Downloaded from https://onlinelibrary.wiley.com/doi/10.1002/pbc.29926 by Universidad Del Pais Vasco, Wiley Online Library on [09/11/2022]. See the Terms and Conditions (https://onlinelibrary.wiley.com/terms-and-conditions) on Wiley Online Library for rules of use; OA articles are governed by the applicable Creative Commons License

Signaling in a Neurofibromatosis 1 Astrocytoma. *J Neuropathol Exp Neurol*. 2000;59(9):759-767.
49. Ratner N, Miller SJ. A RASopathy gene commonly mutated in cancer: the neurofibromatosis type 1 tumour suppressor. *Nat Rev Cancer*. 2015;15(5):290-301.
50. Liu J, Gallo RM, Khan MA, Renukaradhya GJ, Brutkiewicz RR. Neurofibromin 1 impairs natural killer T-cell-dependent antitumor immunity against a T-cell lymphoma. *Front Immunol*. 2018;8:1901.
51. Broux M, Prieto C, Demeyer S, et al. Suz12 inactivation cooperates with JAK3 mutant signaling in the development of T-cell acute lymphoblastic leukemia. *Blood*. 2019;134(16):1323-1336.
52. Jin LH, Choi JK, Kim B, et al. Requirement of split ends for epigenetic regulation of Notch signal-dependent genes during infection-induced hemocyte differentiation. *Mol Cell Biol*. 2009;29(6):1515-1525.
53. Aster JC, Blacklow SC, Pear WS. Notch signalling in T-cell lymphoblastic leukaemia/lymphoma and other haematological malignancies. *J Pathol*. 2011;223(2):263-274.
54. Guo Y, Bao Y, Guo D, Yang W. Pregnancy-associated plasma protein a in cancer: expression, oncogenic functions and regulation. *Am J Cancer Res*. 2018;8(6):955-963.
55. Wang X, Huang H, Young KH. The PTEN tumor suppressor gene and its role in lymphoma pathogenesis. *Aging (Albany NY)*. 2015;7(12):1032.
56. Cao Q, Wang X, Zhao M, et al. The central role of EED in the orchestration of polycomb group complexes. *Nat Commun*. 2014;5:3127.
57. Chen Y, Williams BR. The role of NF-kB in the regulation of the expression of wilms tumor suppressor gene WT1. *Gene Expr*. 2000;9(3):103-114.
58. Oliveira ML, Akkapeddi P, Ribeiro D, Melão A, Barata JT. IL-7R-mediated signaling in T-cell acute lymphoblastic leukemia: an update. *Adv Biol Regul*. 2019;71:88-96.
59. Mcrae HM, Garnham AL, Hu Y, et al. PHF6 regulates hematopoietic stem and progenitor cells and its loss synergizes with expression of TLX3 to cause leukemia. *Blood*. 2019;133(16):1729-1741.
60. Sood R, Kamikubo Y, Liu P. Role of RUNX1 in hematological malignancies. *Blood*. 2017;129(15):2070-2082.
61. Tremblay CS, Brown FC, Collett M, et al. Loss-of-function mutations of dynamin 2 promote T-ALL by enhancing IL-7 signalling. *Leukemia*. 2016;30(10):1993-2001.
62. Pandzic T, Rendo V, Lim J, et al. Somatic PRDM2 c.4467delA mutations in colorectal cancers control histone methylation and tumor growth. *Oncotarget*. 2017;8(58):98646-98659.
63. Xie W, Li X, Chen X, Huang S, Huang S. Decreased expression of PRDM2 (RIZ1) and its correlation with risk stratification in patients with myelodysplastic syndrome. *Br J Haematol*. 2010;150(2):242-244.
64. Jiang L, Gu ZHH, Yan ZXX, et al. Exome sequencing identifies somatic mutations of DDX3X in natural killer/T-cell lymphoma. *Nat Genet*. 2015;47(9):1061–1066.
65. Chauhan PS, Bhushan B, Mishra AK, et al. Mutation of FLT3 gene in acute myeloid leukemia with normal cytogenetics and its association with clinical and immunophenotypic features. *Med Oncol*. 2011;28(2):544-551.
66. Pike KA, Tremblay ML. TC-PTP and PTP1B: regulating JAK-STAT signaling, controlling lymphoid malignancies. *Cytokine*. 2016;82:52-57.
67. Kleppe M, Tousseyn T, Geissinger E, et al. Mutation analysis of the tyrosine phosphatase PTPN2 in Hodgkin's lymphoma and T-cell non-Hodgkin's lymphoma. *Haematologica*. 2011;96(11):1723-1727.
68. Stief SM, Sabrina A, li H, Raphael W, et al. Loss of KDM6A confers drug resistance in acute myeloid leukemia. *Leukemia*. 2020;34(1):50-62.
69. Kim M, Morales LD, Jang I-S, Cho Y-Y, Kim DJ. Protein tyrosine phosphatases as potential regulators of STAT3 signaling. *Int J Mol Sci*. 2018;19(9):2708.
70. Veeriah S, Brennan C, Meng S, et al. The tyrosine phosphatase PTPRD is a tumor suppressor that is frequently inactivated and mutated in glioblastoma and other human cancers. *Proc Natl Acad Sci U S A*. 2009;106(23):9435-9440.
71. Quivoron C, Couronné L, Della Valle V, et al. TET2 inactivation results in pleiotropic hematopoietic abnormalities in mouse and is a recurrent event during human lymphomagenesis. *Cancer Cell*. 2011;20(1):25-38.
72. Wang X, Gao P, Lin F, et al. Wilms' tumour suppressor gene 1 (WT1) is involved in the carcinogenesis of Lung cancer through interaction with PI3K/Akt pathway. *Cancer Cell Int*. 2013;13(114).
73. Morrison DJ, Kim MKH, Berkofsky-Fessler W, Licht JD. WT1 induction of mitogen-activated protein kinase phosphatase 3 represents a novel mechanism of growth suppression. *Mol cancer Res*. 2008;6(7):1225-1231.
74. Kramer A, Kothari A, Wilson W, et al. Dnmt3a regulates T-cell development and suppresses T-ALL transformation. *Leukemia*. 2017;31(11):2479-2490.

SUPPORTING INFORMATION

Additional supporting information can be found online in the Supporting Information section at the end of this article.

How to cite this article: Salmerón-Villalobos J, Ramis-Zaldivar JE, Balagué O, et al. Diverse mutations and structural variations contribute to Notch signaling deregulation in paediatric T-cell lymphoblastic lymphoma. *Pediatr Blood Cancer*. 2022;69:e29926. https://doi.org/10.1002/pbc.29926

15455017, 2022, 11, Downloaded from https://onlinelibrary.wiley.com/doi/10.1002/pbc.29926 by Universidad Del Pais Vasco, Wiley Online Library on [09/11/2022]. See the Terms and Conditions (https://onlinelibrary.wiley.com/terms-and-conditions) on Wiley Online Library for rules of use; OA articles are governed by the applicable Creative Commons License